Thermal Enhancement of Cotunneling in Ultra-Small Tunnel Junctions

T. M. Eiles,[a] G. Zimmerli, H. D. Jensen,[b] and John M. Martinis
National Institute of Standards and Technology, Boulder, Colorado 80303
(Received 21 January 1992)

We have measured the cotunneling current below the Coulomb blockade threshold in a circuit of two ultra-small metallic tunnel junctions. The thermal enhancement of cotunneling, as well as the island-charge dependence, is in excellent agreement with theory. Circuit parameters were measured enabling theoretical and experimental values for the cotunneling current to be compared without adjustable parameters. This comparison yielded agreement within the 15% uncertainty of the experiment. Data showing the cotunneling current near the threshold voltage are also presented.

PACS numbers: 73.40.Gk, 73.40.Rw

The tunneling of electrons through nanoscale junctions is strongly affected by the Coulomb blockade, which inhibits tunneling below a certain threshold voltage [1]. Circuits based on this effect have recently demonstrated the controllable transfer of single electrons between conductive islands [2,3]. The "orthodox theory" of such circuits assumes that an electron tunnels across one junction at a time. However, higher-order perturbation theory shows that tunneling processes can occur in which different electrons simultaneously tunnel across more than one tunnel junction. These processes, called inelastic cotunneling or macroscopic quantum tunneling of charge [4], are crucially important for understanding the operation of circuits as they limit the certainty with which electrons can be manipulated.

Cotunneling rates have been measured in two- and three-junction circuits for normal-metal tunnel junctions [5]. Theoretical predictions that the cotunneling rate scales as V^3 and as the product of the junction conductances have been verified for the double junction [5]. Thermal enhancement of cotunneling [6] has been verified in a 2D electron gas system, but the measurement deviated from theory in that the effective temperature was significantly higher than the bath temperature [7]. In these two experiments [5,7], the magnitude of the cotunneling current could be compared to theory only within a factor of 2–3 due to the uncertainties of the experimental parameters.

In this Letter, we provide a more accurate test of the cotunneling theory. We have measured experimental parameters well enough that the magnitude of the cotunneling current can be accurately compared with theoretical predictions. We also present the first experimental data which show the dependence of cotunneling on bias charge as well as the cotunneling current near the threshold voltage. This latter measurement is of particular interest because the cotunneling prediction diverges logarithmically at the threshold voltage and theorists are now extending their predictions to this region [8,9].

The two-junction circuit model is drawn in Fig. 1, where the boxed symbols represent tunnel junctions with capacitances and resistances of C_1, C_2, R_1, and R_2. We define the quantities $C_\Sigma = C_1 + C_2 + C_g$, $\alpha_1 = (C_2 + C_g)/C_\Sigma$, $\alpha_2 = 1 - \alpha_1 = C_1/C_\Sigma$, $q = C_g V_g/e - 1/2$, $v = V/(e/C_\Sigma)$, and $t = k_B T/(e^2/C_\Sigma)$, where e is the electronic charge and k_B is the Boltzmann constant. All predictions for the current I are periodic in q with period 1.

At temperature $T = 0$, the predicted current for single-junction transitions (no cotunneling) is zero for $|V| < V_t$. For positive V the threshold voltage is $V_t(q) = \max(qe/\alpha_1 C_\Sigma, -qe/\alpha_2 C_\Sigma)$ for $-\alpha_2 < q < \alpha_1$. Above the threshold voltage, the current can be computed by a master equation [1]. For small temperatures $t \lesssim \frac{1}{10}$ and for small enough positive voltages $V < \min[(q+1)e/\alpha_1 C_\Sigma, (1-q)e/\alpha_2 C_\Sigma]$, the master equation reduces to

$$I = \frac{e}{C_\Sigma}\left[R_1 \frac{1-\exp[-(\alpha_1 v - q)/t]}{\alpha_1 v - q} + R_2 \frac{1-\exp[-(\alpha_2 v + q)/t]}{\alpha_2 v + q}\right]^{-1} \quad (1)$$

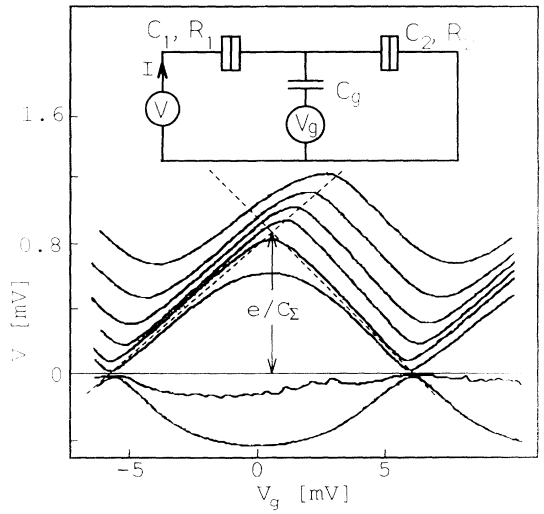

FIG. 1. Plot of measured junction voltage V vs gate voltage V_g taken at eight values of current bias I. From bottom to top the values of current are −15, −1, 44, 145, 332, 555, 849, and 1231 pA. Dashed lines are computed threshold voltages. The refrigerator temperature is 35 mK. Inset: The circuit model for the double-junction system.

for $-\alpha_2 < q < \alpha_1$. The current predicted in Eq. (1) arises from sequential tunneling events through the two junctions, where the denominator represents the sum of the mean times of tunneling for the two junctions. A further useful formula is obtained when $V \approx V_t$, and one of the tunneling times is long and thus dominates the expression. In this limit and when $0 < q < \alpha_1$,

$$I \approx \frac{\alpha_1 (V - V_t)/R_1}{1 - \exp[-\alpha_1 e(V - V_t)/k_B T]}, \quad V \approx V_t . \tag{2}$$

The predicted current for $\alpha_2 < q < 0$ and $V \approx V_t$ is given by Eq. (2) with $R_1, \alpha_1 \rightarrow R_2, \alpha_2$.

Cotunneling theory [4] predicts a finite current for $V < V_t$. At zero temperature and $0 < q < 1$ it predicts

$$I_{ct} = \frac{R_K}{(2\pi)^2 R_1 R_2} \left\{ \left[1 + \frac{2}{u_1 + u_2 + u_1 u_2} \right] \ln[(1+u_1)(1+u_2)] - 2 \right\} V , \tag{3}$$

where $u_1 = V/(qe/C_\Sigma - \alpha_1 V)$, $u_2 = V/[(1-q)e/C_\Sigma - \alpha_2 V]$, and $R_K = h/e^2$. For finite temperatures and small voltages, the result valid for $0 < q < 1$ is [6]

$$I_{ct} = \frac{R_K}{24\pi^2 R_1 R_2} \left[\frac{1}{q(1-q)} \right]^2 \frac{[(2\pi k_B T/e)^2 + V^2] V}{(e/C_\Sigma)^2} . \tag{4}$$

Equation (4) agrees with Eq. (3) for $T = 0$ within 15% for $V < 0.6 V_t$.

Our tunnel junctions were fabricated using electron-beam lithography and double-angle evaporation [10]. The dimension of the metallic island between the aluminum tunnel junctions was 0.5×1.0 μm^2, and the film thicknesses were 30 and 60 nm. The aluminum was driven normal by placing a small permanent magnet next to the sample. Current-voltage measurements were made in a dilution refrigerator with several filter elements placed in the measurement leads [11] to prevent noise from entering the circuit. Junctions with very low capacitance, about 0.1 fF, were deliberately chosen in this experiment to make the reduced temperature t as small as possible. The junction resistances were low enough to produce a measurable cotunneling current, but large enough that cotunneling does not significantly affect the measurement of the junction parameters using data above V_t.

The junction parameters are measured by comparing the characteristics of the device above threshold to the orthodox theory. We think the way our measurements are made is not sensitive to small corrections that come from cotunneling and the environment [12]. We think the cotunneling corrections are negligible because at threshold an estimate of the cotunneling current $I_{ct} \sim 2R_K(e/C_\Sigma)/3\pi^2 R_1 R_2$ from Eq. (4) gives a current smaller than that used to measure the parameters, and it is thought [9] that the cotunneling current goes to zero at voltages slightly above the threshold voltage; we show that our data are consistent with this assumption. The gate capacitance $C_g = 13.9 \pm 0.1$ aF is measured from the periodicity $\Delta V_g = e/C_g$ of the current on the gate voltage. The junction capacitances are measured from the dependence of V_t on V_g. Equation (1) and numerical simulations indicate that for $t \lesssim \frac{1}{10}$ and V slightly larger than V_t, I is closely approximated by a function of $V - V_t$ [see also Eq. (2)]. Thus, a measurement of V vs V_g at constant I yields lines parallel to V_t vs V_g. Such a plot is shown in Fig. 1 for eight values of I. When I is large enough that $V \gtrsim V_t$, the lines form a sawtooth pattern, with the positive and negative slopes independent of I for a large range of I from 145 to 849 pA. The measured slopes and e/C_g then yield the threshold voltage, which is indicated by dashed lines. The capacitances thus obtained are $C_1 = 83.5 \pm 2$ aF, $C_2 = 86.6 \pm 2$ aF, and $e/C_\Sigma = 870 \pm 30$ μV.

The sum of the junction resistances $R_1 + R_2$ is obtained from the differential resistance of the device at voltages $V \sim 10e/C_\Sigma$ well above the threshold voltage. The uncertainty of this measurement arises from the correction due to the electromagnetic environment [13] which has a magnitude less than about 5%. We obtain the ratio of the junction resistances by noting that at $V = e/C_\Sigma$, Eq. (1) reduces to $I = (e/C_\Sigma)/[R_1/(\alpha_1 - q) + R_2/(\alpha_2 + q)]$. At this voltage bias, the q dependence of I has a maximum at $q_{max} = -\alpha_2 + [(R_1/R_2)^{1/2} - 1]/(R_1/R_2 - 1)$. The experimental measurement of q_{max} from I vs V_g data taken at constant voltage e/C_Σ yields $R_2/R_1 = 3.4 \pm 0.4$. Combining this ratio with the measured value $R_1 + R_2$

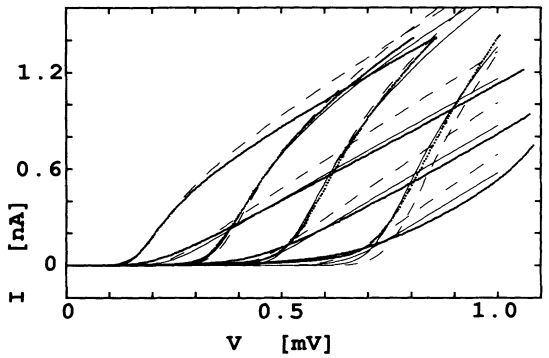

FIG. 2. I-V characteristics at seven values of bias charge. Points are experimental data. Dashed lines are predictions of Eq. (1) using the measured parameters. Solid lines are fitted to the data using parameters $R_1 = 67$ kΩ, $R_2 = 254$ kΩ, $C_1 = 81.5$ aF, $C_2 = 88.6$ aF, $C_g = 13.9$ aF, and $T = 108$ mK. For both sets of theoretical curves the temperature is fitted from the leftmost curve and is higher than the refrigerator temperature 35 mK because of self-heating.

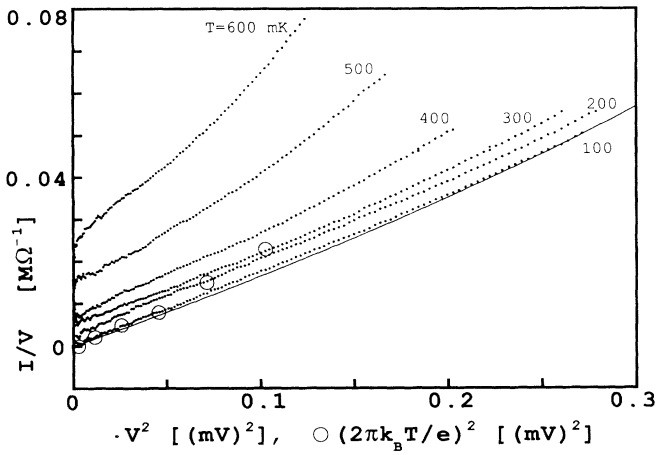

FIG. 3. Plot of I/V vs V^2 for $q=0.55$. Experimental data (solid points) are plotted for six values of T. Open circles are I/V as $V\rightarrow 0$ obtained from the six temperatures plotted vs $(2\pi k_B T/e)^2$. The solid line is the cotunneling prediction of Eq. (3) using the experimentally measured parameters.

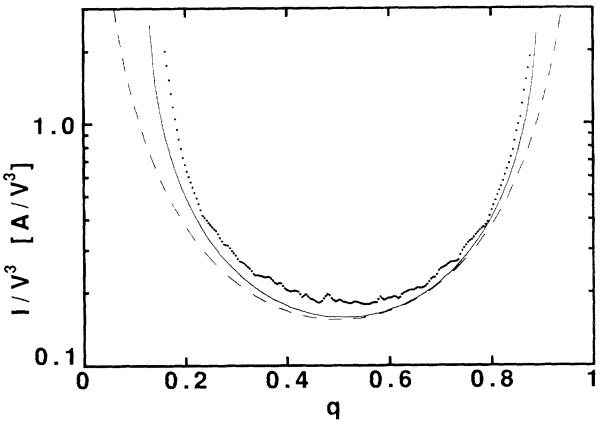

FIG. 4. Plot of I/V^3 vs q for $V=200$ μV and refrigerator temperature 35 mK. Dashed and solid lines are the predictions of Eqs. (3) and (4) based on the measured junction parameters, respectively.

$=292$ k$\Omega\pm 5\%$ gives $R_1=66\pm 9$ kΩ and $R_2=226\pm 29$ kΩ.

As a check on these measurements, we plot in Fig. 2 current-voltage characteristics for the device at seven values of q. Also plotted are predictions of Eq. (1) with our measured parameters and with parameters that were varied for best fit. We find a good fit for values of the parameters which fall within the uncertainties of the measured parameters except for R_1+R_2, which is about 10% too high. However, this high value of R_1+R_2 is consistent with the environmental corrections which are expected to increase at low voltages. We do not expect the data to be fitted exactly by the orthodox theory, especially near threshold, because corrections from the environment and cotunneling are not included. We prefer our measured parameters to our fitted parameters because we think they are less susceptible to systematic errors.

Experimental measurements of the cotunneling current below the threshold voltage are presented in Fig. 3 for $q=0.55$ (maximum V_t) and for temperatures between 100 and 600 mK. We have plotted I/V vs V^2 since Eq. (4) predicts the measurements will fall on a line with a $V=0$ intercept proportional to T^2. The data at the lowest temperature lie on a line. Data at higher temperatures fall parallel to the 100-mK data at low voltages as predicted by Eq. (4), and are displaced upward with increasing temperature. We also plot in Fig. 3 the intercepts of the lines at $V=0$ vs $(2\pi k_B T/e)^2$, as shown by the open circles. Equation (4) predicts that the open circles should also lie on a line with a slope equal to the slope of the lines of the I/V vs V^2 data. The two slopes are approximately equal, confirming that the thermal enhancement term $(2\pi k_B T/e)^2$ of Eq. (4) is correct. Finally, the magnitude of the predicted slope is compared with the data. The solid line in Fig. 4 is the cotunneling prediction; its slope agrees with that of the data to 10%, a value within the uncertainty of $\pm 15\%$ from the measurement of the parameters. The deviation of the higher-temperature data from the predicted line can be accounted for quantitatively by thermally activated single-junction tunneling [e.g., Eq. (1)].

The matrix element in the cotunneling theory incoherently sums over all possible electron-hole excitations, but coherently sums over identical two-junction processes where a transition of either junction 1 or 2 gives the intermediate state. This coherent sum is observed in the q dependence of the cotunneling current. In Fig. 4 the quantity I/V^3 is plotted versus q for $V=200$ μV and for a refrigerator temperature of 35 mK. The cotunneling predictions of Eqs. (3) and (4) are compared with the measurements and show good agreement between the shape of the curves. The small difference between the experiment and theory is accounted for by the uncertainty in the measured parameters.

Joule heating can be an important consideration for experiments on small tunnel junctions [14]. The poor coupling between electrons and phonons at low temperatures [15] predicts that electronic temperatures below about 50–100 mK are difficult to obtain in these devices. Because we focus on cotunneling data above 100 mK, we can reasonably neglect this effect because the thermal enhancement of cotunneling below 100 mK is very small ($<3\%$).

The perturbation theory of cotunneling breaks down as $V\rightarrow V_t$ as evidenced by the logarithmic divergence of Eq. (3). We experimentally investigate this issue with data shown in Fig. 5, where we plot current versus voltage for $q=0.451$ and a temperature $T=200$ mK, high enough that there should be no significant temperature rise due to Joule heating. The prediction of Eq. (1) is plotted as a solid curve, with a measured temperature of 200 mK and junction parameters that yield a best fit between the data

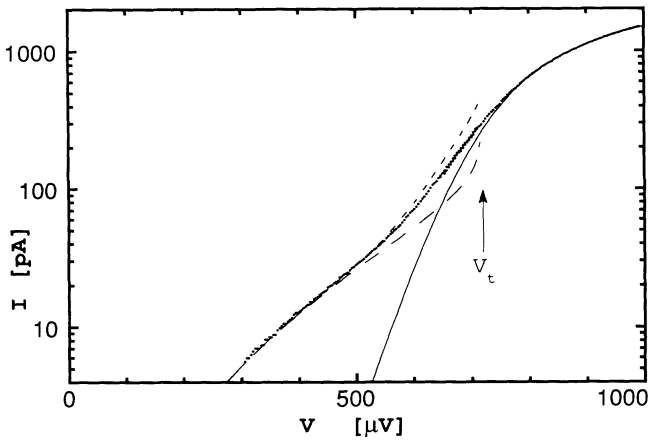

FIG. 5. Current-voltage characteristic taken at $T=200$ mK. The points are experimental data. The solid line is the prediction of Eq. (1) with best-fit parameters $e/C_\Sigma=890$ μV, $\alpha_1=0.56$, $q=0.451$, $R_1=62.8$ kΩ, $R_2=224$ kΩ, and $T=200$ mK. The long-dashed line is the prediction of the cotunneling theory (see text) using the same parameters. The short-dashed line is the sum of the current from the solid and long-dashed lines.

and theory above 800 μV. The prediction of the cotunneling theory for the same parameters is the long-dashed curve, where we have multiplied Eq. (3) by the thermal enhancement factor $(2\pi k_B T/eV)^2+1$ of Eq. (4) to account for the small ($<10\%$) effect of temperature on the cotunneling rate. We see a good fit to both theories at voltages above and below the threshold voltage. Also plotted is the short-dashed curve, the sum of the two predictions. Our experimental data are *consistent* with the cotunneling current being smaller than predicted from Eq. (3) at $V \lesssim V_t$ where the thermal current approaches or is greater in magnitude than the cotunneling current, and a small cotunneling current surviving even slightly above V_t. Because we adjusted experimental parameters to obtain a best fit in this figure, we can make no statement that this is the only possible interpretation of the data in this figure.

In conclusion, our data confirm the temperature and q dependence of the cotunneling theory for a double-junction circuit with normal-metal tunnel junctions. With no adjustable parameters, we have confirmed the magnitude of the predicted current to an accuracy of about 15%.

This work was supported in part by the Office of Naval Research under Contract No. N00014-92-F-0003.

---

[a]Also at Physics Department, University of Colorado, Boulder, CO 80309.

[b]Permanent address: Danish Institute of Fundamental Metrology, DK-2800 Lyngby, Denmark.

[1] D. V. Averin and K. K. Likharev, in *Mesoscopic Phenomena in Solids*, edited by B. Al'tshuler, P. Lee, and R. Webb (Elsevier, Amsterdam, 1991), Chap. 6.

[2] L. J. Geerligs, V. F. Anderegg, P. Holweg, J. E. Mooij, H. Pothier, D. Esteve, C. Urbina, and M. H. Devoret, Phys. Rev. Lett. **64**, 2691 (1990).

[3] H. Pothier, P. Lafarge, P. F. Orfila, C. Urbina, D. Esteve, and M. H. Devoret, Europhys. Lett. **17**, 249 (1992).

[4] D. V. Averin and A. A. Odintsov, Phys. Lett. A **140**, 251 (1989).

[5] L. J. Geerligs, D. V. Averin, and J. E. Mooij, Phys. Rev. Lett. **65**, 3037 (1990).

[6] D. V. Averin and Yu. V. Nazarov, Phys. Rev. Lett. **65**, 2446 (1990).

[7] D. C. Glattli, C. Pasquier, U. Meirav, F. I. B. Williams, Y. Jin, and B. Etienne, Z. Phys. B **85**, 375 (1991).

[8] D. Averin (private communication).

[9] D. Esteve (private communication).

[10] T. A. Fulton and G. J. Dolan, Phys. Rev. Lett. **59**, 109 (1987).

[11] J. M. Martinis, M. H. Devoret, and J. Clarke, Phys. Rev. B **35**, 4682 (1987).

[12] Yu. V. Nazarov, Zh. Eksp. Teor. Fiz. **95**, 975 (1989) [Sov. Phys. JETP **68**, 561 (1989)]; M. H. Devoret, D. Esteve, H. Grabert, G.-L. Ingold, H. Pothier, and C. Urbina, Phys. Rev. Lett. **64**, 1824 (1990).

[13] G.-L. Ingold, P. Wyrowski, and H. Grabert, Z. Phys. B **85**, 443 (1991).

[14] H. Pothier, Ph.D. thesis, Docteur de l'Universite Paris 6, 1991 (unpublished).

[15] M. L. Roukes, M. R. Freeman, R. S. Germain, R. C. Richardson, and M. B. Ketchen, Phys. Rev. Lett. **55**, 422 (1985).